

C.3 Study Site FBG3 (frost boil community)

I Location

Name	Location	Latitude	Longitude	Altitude
FBG3	Franklin Bluffs, Arctic North Slope, Alaska, United States of America	69.67445°	-148.720875°	123 m

At an average elevation of 90 m, Franklin Bluffs is located in Subzone D about 1 km west of the Dalton Highway across from the pipeline access road APL/AMS 130 near green mile marker 375. This access road provides parking at the site. Three 10 x 10 m grids, designated dry, mesic, and wet, have been established at this location in 2002. The goniometer measurements have been carried out next to the moist / zonal site (FB_m/z). [Barreda *et al.*, 2006]

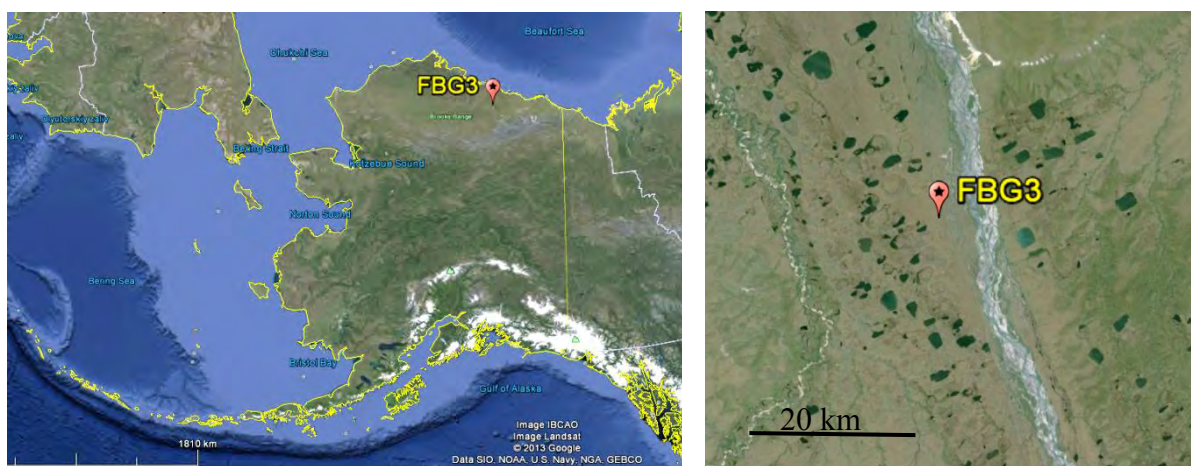


Figure C.3-1: Location of study site FBG3 in Alaska, USA. Source: Google Earth, 2013



Figure C.3-2: Aerial photo of a 10 x 10 m zonal grid at the Franklin Bluffs study location near the FBG3 site. Source: [Barreda *et al.*, 2006]

II Main Vegetation Description

The vegetation at the mesic Franklin Bluffs study location corresponds to the zonal vegetation in subzone D. The zonal plant community of bioclimate subzone D in northern Alaska is *Dryado integrifoliae-Caricetum bigelowii* [Walker et al., 2005], also called moist non-acidic tundra (MNT), or ‘nontussock sedge, dwarf-shrub, moss tundra’ [Walker et al., 2005]. It occurs on circumneutral to basic soils in association with silty loess that is blown from the major rivers in the eastern part of the Arctic Coastal Plain. The average soil pH of this plant community at Franklin Bluffs is 7.9; the average volumetric soil moisture of the top mineral horizon is 45 %, and average depth of thaw by late summer is 40 cm [Kade et al., 2005]. The dominant plants in MNT are sedges (*Carex bigelowii*, *Eriophorum angustifolium* ssp. *triste*, *C. membranacea*, *C. scirpoidea*, *E. vaginatum*), prostrate and hemi-prostrate evergreen dwarf shrubs (*Dryas integrifolia*, *Cassiope tetragona*), prostrate dwarf deciduous shrubs (*Salix arctica*, *S. reticulata*, *Arctous rubra*), scattered erect dwarf deciduous shrubs (*Salix lanata*, *S. glauca*), several forbs (*Papaver macounii*, *Pedicularis lanata*, *Saussurea angustifolia*, *Senecio atropurpureus*, *Pedicularis capitata*, *Polygonum viviparum*, *Cardamine hyperborea*, *Astragalus umbellatus*), mosses (*Tomentypnum nitens*, *Hylocomium splendens*, *Aulacomnium turgidum*, *Rhytidium rugosum*, *Hypnum bambergeri*, *Distichium capillaceum*, *Ditrichum flexicaule*), and lichens (*Thamnolia subuliformis*, *Cetraria* spp.).

An important component of the MNT is the abundant nonsorted circles, also called frost boils, which are small patterned ground features caused by soil frost heave [Walker et al., 2008; Washburn, 1980]. These features cover large parts of most MNT surfaces. The 10 x 10 m zonal grid at Franklin Bluffs has about 30 % cover of nonsorted circles. These features have drier plant communities than the mesic zonal plant communities between the circles, with high cover of lichens and bare soil.

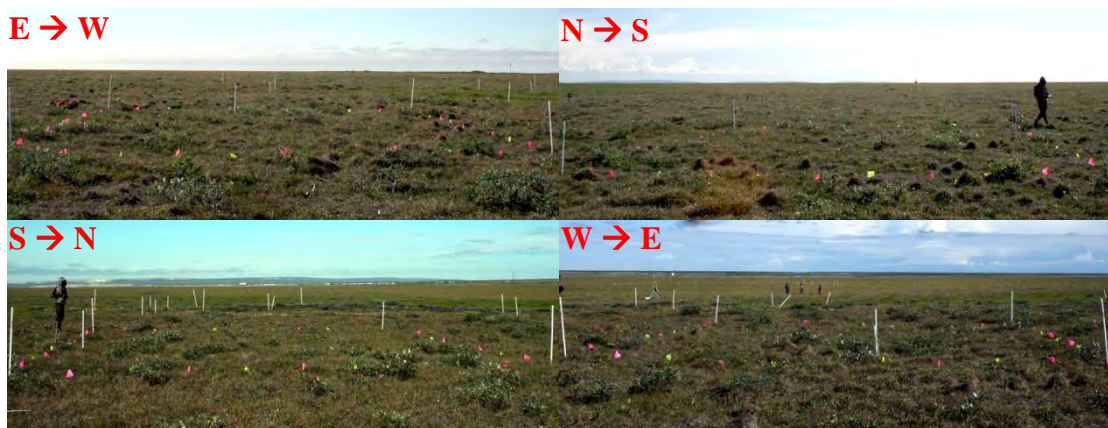


Figure C.3-3: Overview images of MNT tundra at the mesic Franklin Bluffs study location near the FBG3 site. Source: [Buchhorn and Schwieder, 2012]

III *Vegetation Description of the FBG3 Site*

The focus of the measurements at this goniometer site has been a frost boil community (*Junco biglumis-Dryadetum integrifoliae pedicularetosum*). The 1 x 1 m plot is homogeneously covered by the nonsorted circles community.



Figure C.3-4: Overview images of the FBG3 vegetation from cardinal directions.



Figure C.3-5: Nadir image of the FBG3 vegetation (frost boil).

IV *Overview of the Spectro-Goniometer Measurements*

Table C.3-1: Overview of the spectro-goniometer measurements at the FBG3 study site.

Name	Day	Starting Time	Duration	SAA	SZA	Sky
FBG3_01	2012-07-13	13:56:00	18 min	181°	48°	cirrostratus

Table C.3-2: Spectro-directional data of the FBG3_01 spectro-goniometer measurement.

FBG3_01 (SA = 48°, SAA = 181°)		Viewing Geometry (Viewing Zenith Angle Viewing Azimuth Angle)																			
		0j0	5180	5202.5	5225	5270	5315	5337.5	5j0	522.5	545	590	5135	5157.5	10180	10190	10202.5	10225	10270	10315	10337.5
HCRF EnMAP blue (479 nm)	0.0435	0.0481	0.0472	0.0456	0.0427	0.0462	0.0424	0.0425	0.0466	0.0419	0.0460	0.0486	0.0460	0.0500	0.0483	0.0511	0.0460	0.0426	0.0465	0.0409	0.0414
HCRF EnMAP green (549 nm)	0.0610	0.0660	0.0620	0.0616	0.0595	0.0644	0.0593	0.0597	0.0647	0.0590	0.0631	0.0665	0.0629	0.0684	0.0671	0.0680	0.0630	0.0601	0.0632	0.0574	0.0576
HCRF EnMAP rot (672 nm)	0.0680	0.0755	0.0738	0.0708	0.0695	0.0723	0.0661	0.0669	0.0744	0.0672	0.0729	0.0751	0.0709	0.0774	0.0769	0.0711	0.0678	0.0723	0.0645	0.0650	0.0650
HCRF EnMAP NIR (864 nm)	0.2281	0.2161	0.1883	0.2034	0.2220	0.2342	0.2108	0.2207	0.2364	0.2121	0.2102	0.2122	0.2009	0.2208	0.2289	0.2081	0.2084	0.2233	0.2277	0.2132	0.2166
ANIF EnMAP rot (672 nm)	1.0000	1.1110	1.0853	1.0424	1.0232	1.0636	0.9722	0.9848	1.0950	0.9881	1.0732	1.1056	1.0426	1.1395	1.1320	1.1751	1.0463	0.9972	1.0633	0.9489	0.9568
ANIF EnMAP NIR (864 nm)	1.0000	0.9558	0.8329	0.8998	0.9819	1.0359	0.9324	0.9763	1.0457	0.9380	0.9298	0.9387	0.8886	0.9767	1.0125	0.9203	0.9220	0.9875	1.0070	0.9432	0.9580
Rel. Blue Absorption Depth	0.2630	0.2464	0.2157	0.2396	0.2616	0.2718	0.2670	0.2764	0.2700	0.2757	0.2527	0.2553	0.2481	0.2446	0.2583	0.2232	0.2451	0.2695	0.2453	0.2776	0.2726
Rel. Red Absorption Depth	0.8957	0.6904	0.5696	0.6989	0.8168	0.8473	0.8207	0.8812	0.8340	0.8256	0.7151	0.6742	0.6968	0.6871	0.7352	0.5918	0.7229	0.8505	0.8136	0.8795	0.8789
NDVI (EnMAP)	0.5377	0.4821	0.4371	0.4834	0.5229	0.5283	0.5227	0.5346	0.5212	0.5190	0.4848	0.4770	0.4785	0.4807	0.4989	0.4453	0.4913	0.5342	0.5181	0.5356	0.5382
Nadir Norm. NDVI (AVHRR)	1.0000	0.9036	0.8326	0.9073	0.9760	0.9814	0.9718	0.9923	0.9745	0.9661	0.9115	0.8911	0.8885	0.8974	0.9308	0.8419	0.9188	0.9938	0.9694	0.9922	1.0058
Nadir Norm. NDVI (MODIS)	1.0000	0.9048	0.8308	0.9072	0.9738	0.9824	0.9732	0.9941	0.9762	0.9668	0.9126	0.8939	0.8915	0.8990	0.9314	0.8410	0.9195	0.9942	0.9690	0.9926	1.0074
Nadir Norm. NDVI (EnMAP)	1.0000	0.8966	0.8128	0.8989	0.9724	0.9824	0.9721	0.9942	0.9692	0.9651	0.9015	0.8871	0.8899	0.8939	0.9240	0.8280	0.9136	0.9935	0.9636	0.9960	1.0008

(cont.)

FBG3_01 (SA = 48°, SAA = 181°)		Viewing Geometry (Viewing Zenith Angle Viewing Azimuth Angle)																			
		10j0	1010	1022.5	1045	1090	10135	10157.5	10170	20180	20190	20202.5	20225	20270	20315	20337.5	20350	20j0	2010	2022.5	2045
HCRF EnMAP blue (479 nm)	0.0404	0.0419	0.0456	0.0417	0.0489	0.0490	0.0515	0.0487	0.0583	0.0576	0.0591	0.0517	0.0417	0.0437	0.0406	0.0408	0.0377	0.0378	0.0377	0.0398	0.0434
HCRF EnMAP green (549 nm)	0.0567	0.0592	0.0633	0.0583	0.0661	0.0679	0.0701	0.0689	0.0798	0.0801	0.0795	0.0710	0.0601	0.0607	0.0559	0.0561	0.0519	0.0534	0.0533	0.0554	0.0620
HCRF EnMAP rot (672 nm)	0.0644	0.0665	0.0729	0.0666	0.0775	0.0754	0.0807	0.0770	0.0902	0.0888	0.0913	0.0825	0.0675	0.0677	0.0637	0.0645	0.0589	0.0587	0.0600	0.0629	0.0678
HCRF EnMAP NIR (864 nm)	0.2149	0.2294	0.2356	0.2093	0.2129	0.2254	0.2221	0.2211	0.2476	0.2566	0.2418	0.2323	0.2336	0.2276	0.2045	0.2066	0.1956	0.2098	0.2193	0.2033	0.2176
ANIF EnMAP rot (672 nm)	0.9477	0.9789	1.0725	0.9799	1.1404	1.1094	1.1871	1.1329	1.2777	1.3060	1.3438	1.2135	0.9829	0.9861	0.9372	0.9496	0.8668	0.8637	0.8823	0.9253	0.9678
ANIF EnMAP NIR (864 nm)	0.9507	1.0146	1.0422	0.9259	0.9416	0.9971	0.9826	0.9779	1.0950	1.1350	1.0696	1.0277	1.0334	1.0069	0.9048	0.9095	0.8651	0.9700	0.8991	0.9625	0.9625
Rel. Blue Absorption Depth	0.2715	0.2853	0.2882	0.2696	0.2408	0.2632	0.2468	0.2480	0.2440	0.2538	0.2327	0.2555	0.2877	0.2572	0.2696	0.2652	0.2634	0.2716	0.2681	0.2703	0.2777
Rel. Red Absorption Depth	0.8922	0.9381	0.8524	0.8125	0.6523	0.7354	0.6603	0.7039	0.6511	0.7059	0.6168	0.6787	0.9157	0.8999	0.8453	0.8322	0.8755	0.9711	0.9990	0.8515	0.8307
NDVI (EnMAP)	0.5388	0.5503	0.5275	0.5173	0.4682	0.4987	0.4671	0.4833	0.4857	0.4860	0.4517	0.4760	0.5518	0.5415	0.5251	0.5222	0.5370	0.5627	0.5705	0.5274	0.5248
Nadir Norm. NDVI (AVHRR)	1.0075	1.0228	0.9840	0.9661	0.8831	0.9252	0.8709	0.9019	0.8494	0.8949	1.0229	1.0070	0.9825	1.0070	0.9825	0.9812	1.0042	1.0430	1.0607	0.9803	0.9742
Nadir Norm. NDVI (MODIS)	1.0075	1.0238	0.9855	0.9674	0.8833	0.9287	0.8733	0.9035	0.8725	0.9037	0.8499	0.8947	1.0239	1.0093	0.9835	0.9820	1.0061	1.0463	1.0630	0.9818	0.9779
Nadir Norm. NDVI (EnMAP)	1.0021	1.0235	0.9809	0.9620	0.8669	0.9274	0.8687	0.8989	0.8661	0.9037	0.8401	0.8853	1.0261	1.0071	0.9765	0.9712	0.9987	1.0465	1.0611	0.9809	0.9760

(cont.)

FBG3_01 (SA = 48°, SAA = 181°)		Viewing Geometry (Viewing Zenith Angle Viewing Azimuth Angle)																			
		20135	20157.5	20170	30180	30190	30202.5	30225	30270	30315	30337.5	30350	30j0	3010	30122.5	3045	30190	30135	30157.5	30170	30190
HCRF EnMAP blue (479 nm)	0.0537	0.0598	0.0602	0.0702	0.0682	0.0666	0.0558	0.0397	0.0399	0.0377	0.0378	0.0355	0.0368	0.0408	0.0446	0.0400	0.0460	0.0674	0.0676	0.0676	0.0676
HCRF EnMAP green (549 nm)	0.0758	0.0827	0.0843	0.0977	0.0915	0.0902	0.0778	0.0588	0.0557	0.0562	0.0522	0.0520	0.0490	0.0512	0.0568	0.0639	0.0866	0.0946	0.0966	0.0966	0.0966
HCRF EnMAP rot (672 nm)	0.0838	0.0947	0.0960	0.1092	0.1020	0.1031	0.0877	0.0631	0.0637	0.0631	0.0592	0.0594	0.0581	0.0648	0.0676	0.0954	0.1062	0.1062	0.1054	0.1054	0.1054
HCRF EnMAP NIR (864 nm)	0.2570	0.2588	0.2708	0.2998	0.2756	0.2632	0.2513	0.2475	0.2169	0.2190	0.1995	0.1948	0.1857	0.2030	0.2091	0.2252	0.2807	0.2940	0.3014	0.3014	0.3014
ANIF EnMAP rot (672 nm)	1.2332	1.3933	1.4125	1.6062	1.5005	1.5169	1.2907	0.9285	0.9377	0.9289	0.8713	0.8735	0.8146	0.8543	0.9536	0.9943	1.4041	1.5620	1.5509	1.5509	1.5509
ANIF EnMAP NIR (864 nm)	1.1368	1.1448	1.1979	1.3261	1.2191	1.1643	1.1114	1.0950	0.9595	0.9688	0.8825	0.8615	0.8215	0.8979	0.9247	0.9963	1.2415	1.3004	1.3330	1.3330	1.3330
Rel. Blue Absorption Depth	0.2774	0.2666	0.2689	0.2603	0.2521	0.2375	0.2584	0.3157	0.2737	0.2815	0.2585	0.2535	0.2581	0.2614	0.2720	0.2763	0.3037	0.2743	0.2743	0.2827	0.2827
Rel. Red Absorption Depth	0.7732	0.6630	0.7002	0.6666	0.6431	0.5797	0.7007	1.0856	0.9123	0.9438	0.8977	0.8557	0.8767	0.9321	0.8601	0.8800	0.7420	0.6740	0.6740	0.7042	0.7042
NDVI (EnMAP)	0.5081	0.4643	0.4766	0.4662	0.4598	0.4371	0.4824	0.5937	0.5458	0.5525	0.5422	0.5328	0.5407	0.5552	0.5287	0.5384	0.4925	0.4694	0.4694	0.4817	0.4817
Nadir Norm. NDVI (AVHRR)	0.9418	0.8689	0.8842	0.8659	0.8553	0.8172	0.8964	1.0866	1.0156	1.0263	1.0139	1.0016	1.0106	1.0327	0.9823	0.9940	0.9101	0.8756	0.8900	0.8900	0.8900
Nadir Norm. NDVI (MODIS)	0.9461	0.8715	0.8855	0.8664	0.8564	0.8190	0.8983	1.0899	1.0185	1.0294	1.0153	1.0023	1.0135	1.0345	0.9846	0.9986	0.9151	0.8780	0.8937	0.8937	0.8937
Nadir Norm. NDVI (EnMAP)	0.9450	0.8634	0.8863	0.8669	0.8551	0.8129	0.8972	1.1042	1.0151	1.0274	1.0084	0.9908	1.0056	1.0324	0.9795	1.0013	0.9160	0.8729	0.8959	0.8959	0.8959

V Main Spectral Characteristics

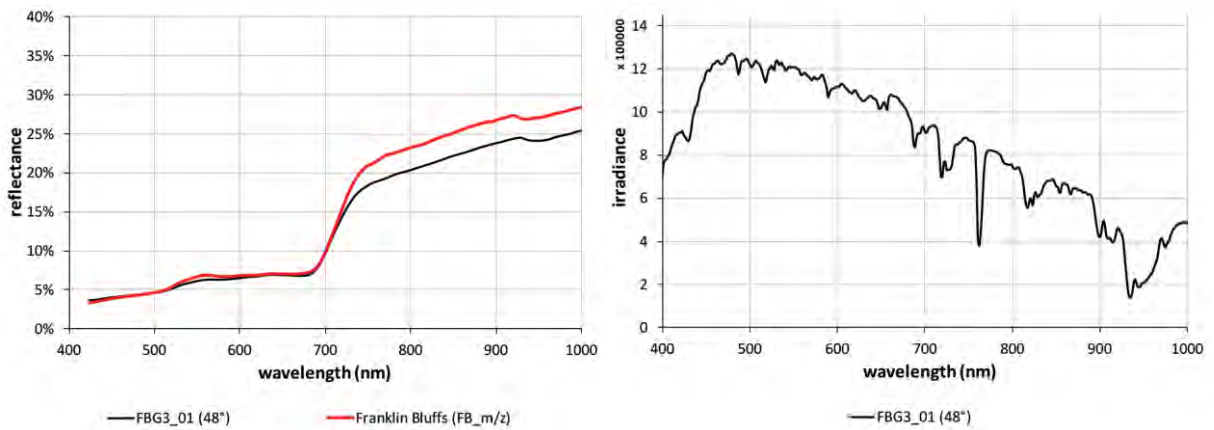


Figure C.3-6: Nadir reflectances and irradiance profiles of the FBG3 site. Left: Comparison of the nadir reflectance signatures with the average zonal vegetation (MNT). Right: Comparison of the total irradiance profiles.

VI HCRF Visualization

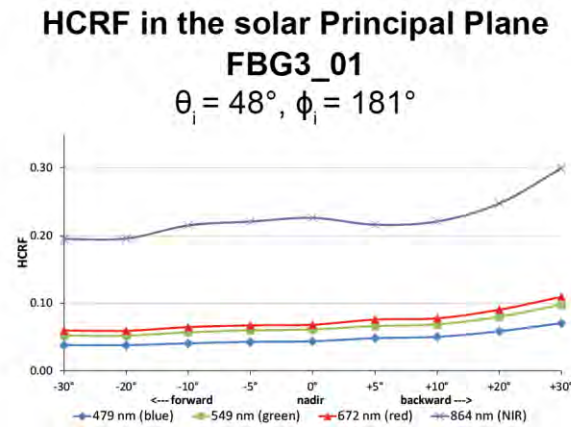


Figure C.3-7: Comparison of the HCRF values at 479 nm (blue), 549 nm (green), 672 nm (red), and 864 nm (NIR) in the solar principal plane of the FBG3 site.

Changes in irradiance



Figure C.3-8: Legend of the outlier indicator graphics shown in Figure C.3-9, C.3-10, and C.3-13

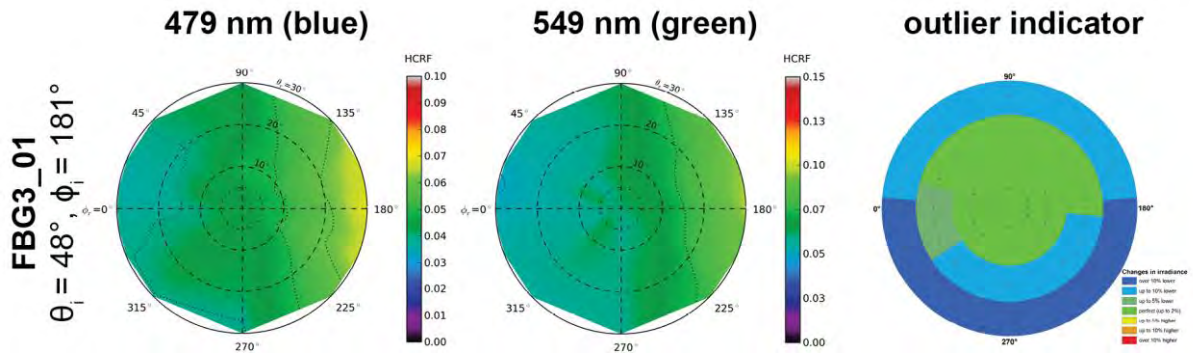


Figure C.3-9: HCRF visualization at 479 nm and 549 nm of the FBG3 site.

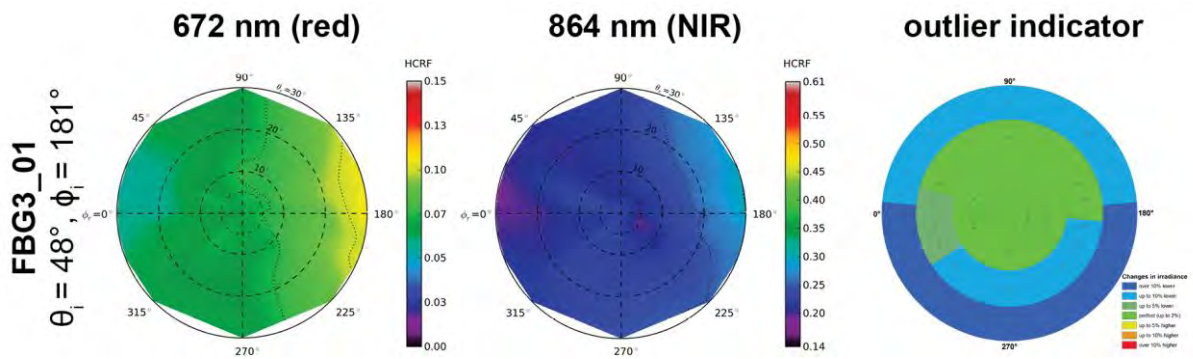


Figure C.3-10: HCRF visualization at 672 nm and 864 nm of the FBG3 site.

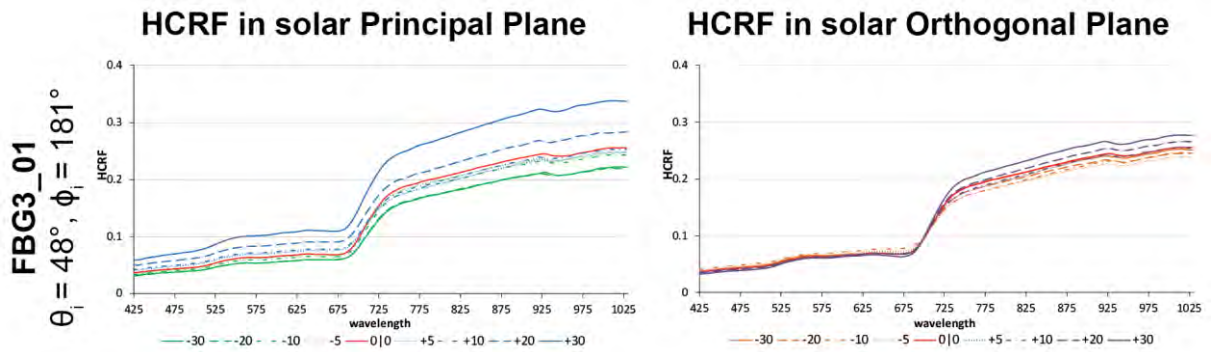


Figure C.3-11: HCRF visualization in principal & orthogonal plane of the FBG3 site.

VII ANIF Visualization

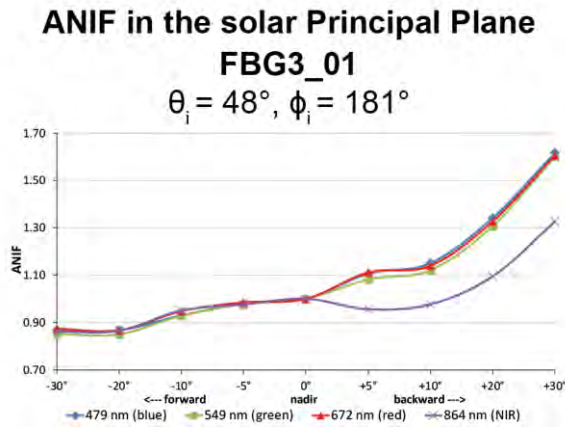


Figure C.3-12: Comparison of the ANIF values at 479 nm (blue), 549 nm (green), 672 nm (red), and 864 nm (NIR) in the solar principal plane of the FBG3 site.

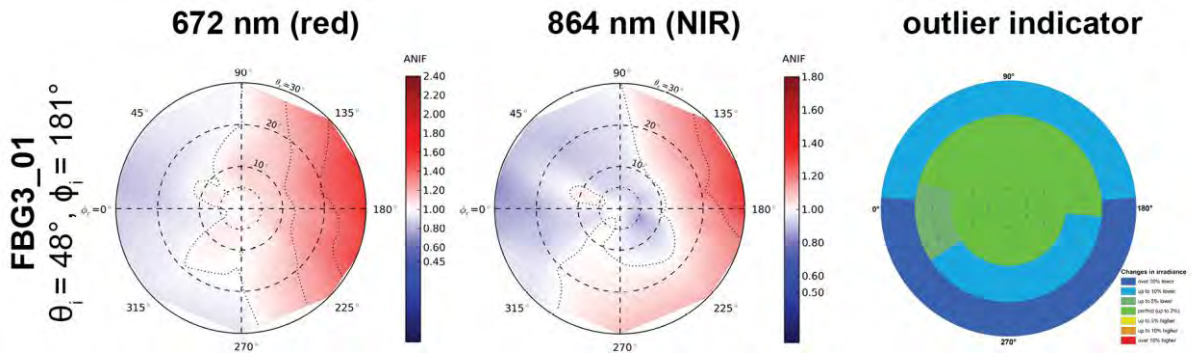


Figure C.3-13: ANIF visualization at 672 nm and 864 nm of the FBG3 site.

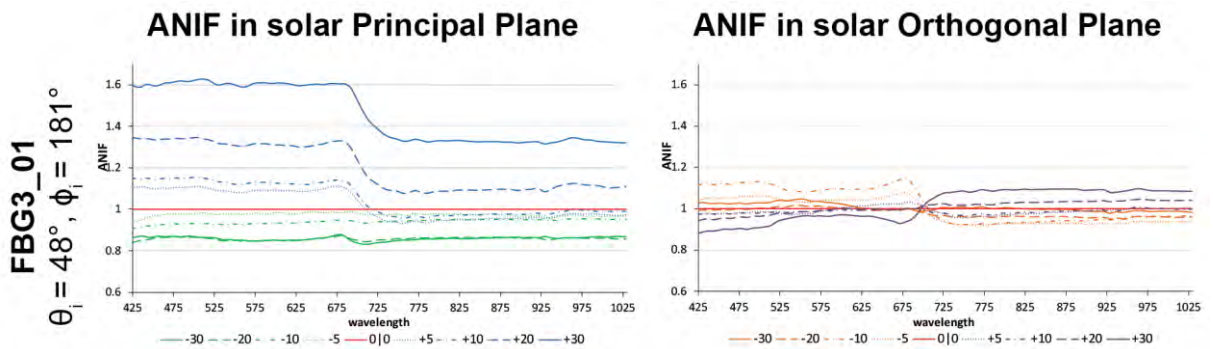


Figure C.3-14: ANIF visualization in principal & orthogonal plane of the FBG3 site.

VIII ANIX Visualization

ANIX in the solar Principal and Orthogonal Plane

FBG3_01

$\theta_i = 48^\circ, \phi_i = 181^\circ$

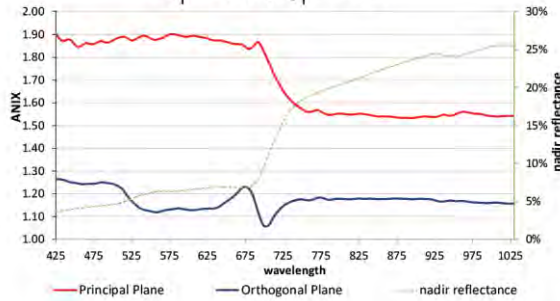


Figure C.3-15: Comparison of the ANIX in the solar principal and orthogonal plane with the nadir reflectance of the FBG3 site.

IX NDVI and Relative Absorption Depth Visualization

NDVI in the solar Principal and Orthogonal Plane

FBG3_01

$\theta_i = 48^\circ, \phi_i = 181^\circ$

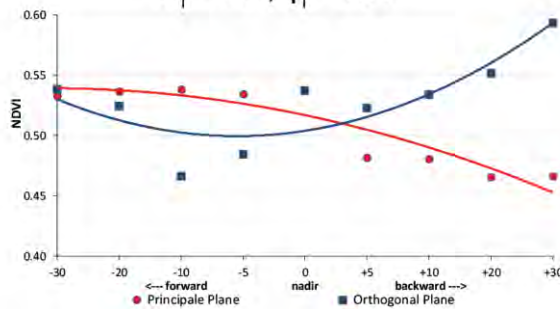


Figure C.3-16: Comparison of the NDVI in the solar principal and orthogonal plane of the FBG3 site.

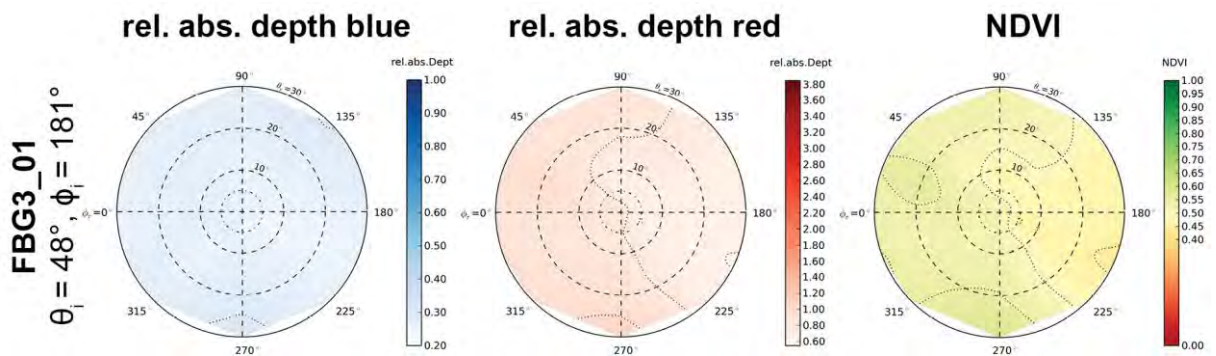


Figure C.3-17: Visualization of relative absorption depth & NDVI of the FBG3 site.

X NDVI Comparison of Different Sensors

Table C.3-3: Center wavelengths and band widths of the broadband and narrowband NDVIs, based on the spectral response curves of the AVHRR, MODIS and EnMAP sensors.

NDVI	Sensor	Sensor band	Center wavelength (nm)	band width (nm)
NDVI_{AVHRR} [broadband]	AVHRR/3	red: band 1 NIR: band 2	630 865	100 275
NDVI_{MODIS} [broadband]	MODIS	red: band 1 NIR: band 2	645 859	50 35
NDVI_{EnMAP} [narrowband]	EnMAP	red: band 47 NIR: band 73	672 864	6.5 8

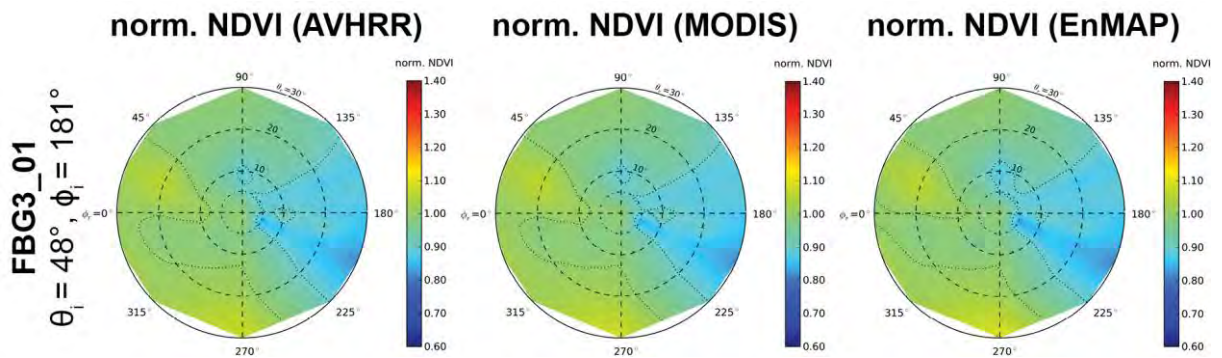


Figure C.3-18: Comparison of AVHRR, MODIS & EnMAP NDVI of the FBG3 site.